

The effect of alloying elements on the dislocation climbing velocity in Ni: A first-principles study

Xiao-Xiang Yu ^{a,*}, Chong-Yu Wang ^{b,c}

^a Department of Materials Science and Engineering, Tsinghua University, Beijing 100084, China

^b Department of Physics, Tsinghua University, Beijing 100084, China

^c The International Centre for Materials Physics, Chinese Academy of Sciences, Shenyang 110016, China

Received 24 May 2009; received in revised form 8 August 2009; accepted 9 August 2009

Available online 21 September 2009

Abstract

By using density functional theory calculations in conjunction with the climbing images nudged elastic band method, the effects of alloying elements Re, W, Mo, Cr, Co and Ru on the velocity of dislocation climbing in gamma Ni were studied. The results shed a light on the mechanism of these elements suppressing the dislocation motion by connecting the stacking fault energy and the migration activation energy of vacancy with the dislocation climbing velocity. It is found that the elements can decrease the stacking fault energy of Ni and raise the migration activation energy of vacancy. The changes of these two energies result in the increase of the formation energy and the diffusion activation energy of the jog, thus the dislocation climbing is restricted. The results also reveal that the influences of alloying elements on dislocation climbing velocity depend on the characters of dislocations.

Crown Copyright © 2009 Published by Elsevier Ltd. on behalf of Acta Materialia Inc. All rights reserved.

Keywords: Dislocation dynamics; Nickel alloys; First-principle electron theory

1. Introduction

Single-crystal Ni-based superalloys are unique high-temperature structural materials used in turbine engines because of their outstanding high-temperature strength, ductility and environmental resistance at elevated temperature [1]. The main structure of such alloys is the precipitate of the ordered intermetallic γ' phase with $L1_2$ structure which is coherently embedded in a solid solution matrix of the γ phase. Although many mechanisms can contribute to the high-temperature strength of Ni-based superalloys, the two major strengthening mechanisms are precipitation hardening and solid-solution strengthening [2]. Since the dislocations move primarily in the γ phase during creep deformation, the solid-solution elements in the γ matrix [3] can restrict the movement of dislocation and raise the

high-temperature strength of superalloys. Elements such as Re, W, Mo, Ru, Co and Cr preferentially partition to the matrix [4,5], and improve the stability of the γ phase.

The magnitude of the stacking fault energy (SFE) in γ phase is very important for superalloys because the dislocations, dissociated into their SHOCKLEY partial dislocations, must constrict locally if they are to cross-slip or climb [6]. Since obstacles such as precipitates can be circumvented by this mechanism, widely spaced partial dislocations due to low values of stacking fault energy are advantages for superalloys to resist high-temperature creep deformation. McLean firstly considered the influence of SFE on creep in 1962 [7]. Weertman later suggested that a strong SFE effect on the steady-state creep rate could be expected in high-temperature creep controlled by dislocation climb [8,9]. Dislocations climbing is more difficult than slip and must be helped by diffusion or large stresses because the vacancies or excess matter produced by climb require larger energies [10]. On this basis, besides low values of the stacking fault energy, slow rate of the dislocation

* Corresponding author.

E-mail address: yuxx07@mails.tsinghua.edu.cn (X.-X. Yu).

climbing arising from small diffusion coefficient is also beneficial to high-temperature properties.

Some experiments have confirmed that the SFE of the γ is reduced substantially with the addition of solid-solution elements [11], the effect of the alloying elements on the rate of the diffusion processes has also been reported [12]. However, the mechanism of the alloying elements restricting the dislocation climbing is not yet clear, the influences of these solid-solution elements on stacking fault energy, diffusion coefficient of the matrix and associated dislocation climbing velocity need systematic investigation. In this paper, first-principles calculations were used to study the influence of Re, W, Mo, Ru, Co and Cr on stacking fault energy, the formation energy and migration barrier of vacancy in Ni. These energies have directly relationship with the velocity of dislocation climbing. The dependence of dislocation climbing velocity on the character of dislocation is also discussed based on an extended dislocation model.

The paper is organized as follows: Following the Introduction, Section 2 describes the computational method, model and results for the influence of alloying elements on stacking fault energy. The effects of the alloying elements on the vacancy diffusion are presented in Section 3. Section 4 analyzes the dependence of the dislocation climbing velocity on the addition of alloying elements and the character of dislocation. Finally, a short summary is given in Section 5.

2. The influence of alloying elements on stacking fault energy

2.1. Computational method

The density functional theory calculations were carried out with the plane-wave based Vienna AB Initio Simulation Package (VASP) [13,14] using the projector augmented wave (PAW) method [15,16] and the generalized gradient approximation (GGA) in the parametrization by J.P. Perdew, K. Burke and M. Ernzerhof (PBE) [17]. The spin-polarized GGA (SGGA) was also employed considering the magnetic effects. Plane waves have been included up to a cutoff energy of 270 eV which yields converged results. A realspace projection scheme was used for efficient computations. The convergence accuracy of total energy was chosen as 10^{-4} eV in the relaxation of electronic degrees of freedom. The structures of the models were relaxed until the maximum force was less than 0.02 eV/Å. A $4 \times 4 \times 2$ k -mesh was used for the k points sampling according to Monkhorst–Pack scheme [18].

2.2. Computational model

Ni is the close-packed fcc structure with an arrangement of $\cdots ABCABC \cdots$ along the $\langle 111 \rangle$ direction. In Fig. 1, a C layer was removed resulting in a break in the stacking sequence and formed an intrinsic fault. The models containing both the intrinsic stacking fault and alloying

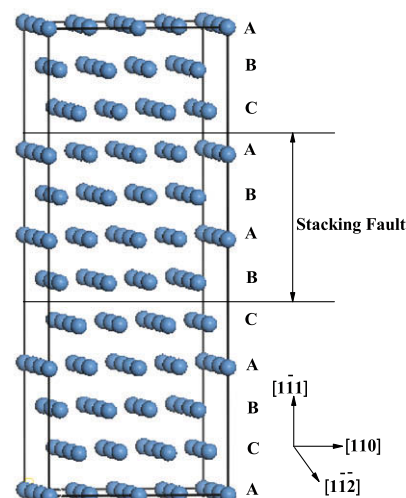


Fig. 1. The intrinsic stacking fault in Ni. The supercell contains ABCABABCABC, totally 11 layers of Ni.

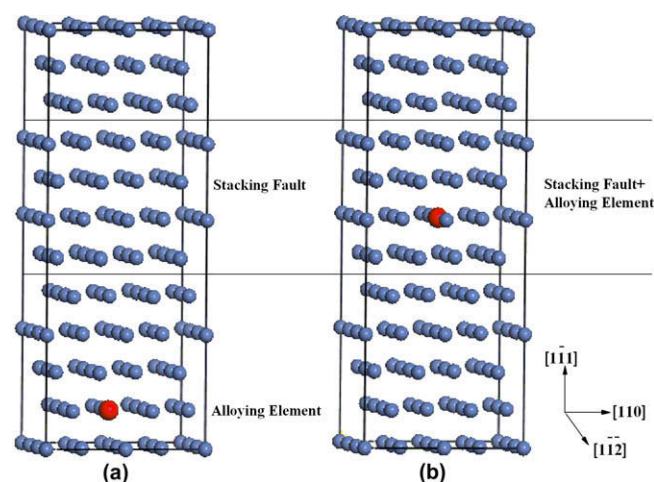


Fig. 2. The supercell containing both the intrinsic stacking fault and alloying element: (a) The alloying element is far from the stacking fault region. (b) The alloying element locates in stacking fault region. The small blue balls stand for Ni atoms and the big red ball stands for alloying element. (For interpretation of the references to colour in this figure legend, the reader is referred to the web version of this article.)

element are shown in Fig. 2. In Fig. 2a, the alloying element is far from the stacking fault (SF) region. In contrast, the alloying element is located in the SF region in Fig. 2b. The three models in Figs. 1 and 2 all contain 11 layers, totally 132 atoms.

2.3. Calculation results and discussion

The change of system energy caused by the stacking fault can be expressed as

$$\Delta E = E_{\text{defect}} - E_{\text{perfect}} \quad (1)$$

where E_{defect} and E_{perfect} are the energies of the systems with and without the stacking fault, respectively. The stacking fault energy per unit area is defined as

$$E_{sf} = \frac{\Delta E}{\Delta S} \quad (2)$$

where ΔS is the area of stacking fault region. Eq. (2) gives the energy needed to form a stacking fault per unit area.

As a benchmark, the calculated stacking fault energy of pure Ni per unit area E_{sf}^{pure} are 125.25 mJ/m² and 130.35 mJ/m² by GGA and spin-polarized GGA(SGGA), respectively, which are in excellent agreement with the available experimental value of 128 mJ/m² [19,20].

The change of stacking fault energy per unit area due to alloying elements is defined as

$$\Delta E_{sf} = \frac{E_{sf}^b(i) - E_{sf}^a(i)}{\Delta S} \quad (3)$$

where $E_{sf}^b(i)$ is the energy of SF system with the alloying element i located in the SF region as shown in Fig. 2b. $E_{sf}^a(i)$ is the energy of SF system with the alloying element i far from the SF region as shown in Fig. 2a.

The calculation results are summarized in Table 1. It can be concluded that under the same concentrations, Mo, Re and W can decrease the stacking fault energy more than Ru and Cr. Co changes the SFE least. The differences between the results calculated by GGA and SGGA suggest that the magnetic effect must be considered in calculations.

In order to explore the mechanisms of the alloying elements reducing the SFE, the electronic charge density differences is plotted in the (111) plane with alloying elements in the center, as presented in Fig. 3. As seen from Fig. 3, more electrons are accumulated around the atom of Re, Mo and W than those around Ru, Cr and no obvious accumulation of electrons around Co. These indicate that the bondings of Re–Ni, W–Ni and Mo–Ni are stronger than those of Ru–Ni, Cr–Ni and Co–Ni. The forming of bondings will reduce the energy of stacking fault region, the stronger the bondings form, the more the SFE decreases. Therefore, Re, Mo and W can reduce SFE more than Ru, Cr and Co.

Besides charge differences, the addition of Re was taken for example and the partial density of states (PDOS) was calculated by means of Lorenz broadening scheme. PDOS (d-DOS) for the central Re and its first nearest neighbor Ni atom are shown in Fig. 4.

From Fig. 4, it can be seen that there exists d–d hybridization between Re and Ni, which results in a strong bonding between Re and Ni. It is easy to understand that Re and Ni mainly interacts by the hybridization of d orbitals,

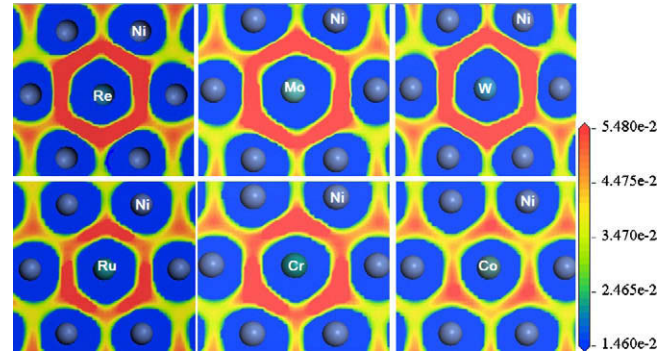


Fig. 3. The electronic charge density difference (in units of e/(a.u.)³) in the (111) plane of Ni, six alloying elements are in the center, respectively.

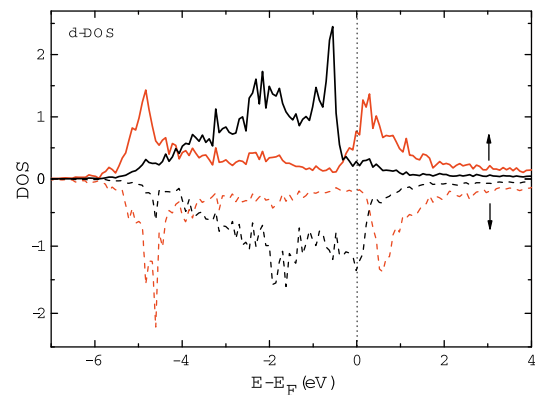


Fig. 4. d-DOS for the central Re and its first nearest neighbor Ni. Red lines are d-DOS of atom Re in the stacking fault region. Black lines are d-DOS of atom Ni which is the first nearest neighbor of Re. The Fermi level is shifted to zero. The d-DOS has two parts, one is spin up (solid line) and the other is spin down (dashed line). (For interpretation of the references to colour in this figure legend, the reader is referred to the web version of this article.)

because most of their valence electrons are from the d orbitals. The bondings of W–Ni and Mo–Ni are also formed by the same mechanism.

3. The influence of alloying elements on vacancy diffusion

3.1. Computational method

Crystal with vacancy and alloying element was modeled using supercells of $3a_0 \times 3a_0 \times 3a_0$ (containing 107 atoms), which were large enough to get converged total energies according to our tests. A $3 \times 3 \times 3$ k -mesh was used for the k points sampling. The alloying element was seated at the center of the supercell, and the vacancy was located in the site of the first nearest neighbor of the alloying element as shown in Fig. 5.

The structure was then relaxed by minimizing the total energy using SGGA method until the maximum force was less than 0.02 eV/Å with the convergence accuracy of 10^{-4} eV in the relaxation of electronic degrees of freedom. In order to get the activation energy of the vacancy diffusion, the climbing image nudged elastic band method

Table 1

The influence of alloying elements on stacking fault energy.

Alloying element	ΔE_{sf} (mJ/m ²)		$E_{sf}^{pure} + \Delta E_{sf}$ (mJ/m ²)	
	GGA	SGGA	GGA	SGGA
Re	−24.91	−22.96	100.34	107.39
Co	−1.16	−6.52	124.09	123.83
W	−22.49	−22.69	102.76	107.66
Cr	−17.28	−10.03	107.97	120.32
Mo	−25.57	−24.85	99.68	105.55
Ru	−17.75	−12.43	107.50	117.92

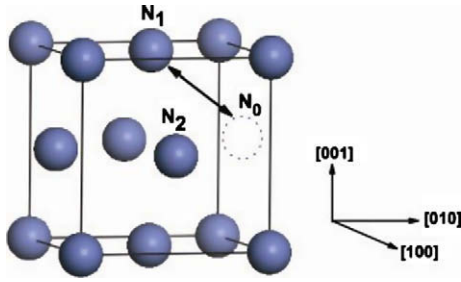


Fig. 5. Diffusion path of vacancy in Ni, the vacancy is represented by circle with dotted line and the arrow denotes the migration paths, the alloying elements substitute the Ni atom at site N_2 .

(CI-NEB) [21,22] as implemented in VASP by Henkelman, Jónsson et al. [23] was used, which is expected to be more reliable than dragging an atom from minimum to minimum across the estimated or guessed saddle. Three images were used in the computations to determine the minimum energy path and the reliability of a small number of images was confirmed. The images were relaxed until the maximum residual force was less than 0.02 eV/\AA .

3.2. Calculation results and discussion

3.2.1. Vacancy formation energy

The vacancy formation energy is the energy required to take an atom from inside the crystal, and place it into a reservoir of the same atoms. It is defined that

$$E_{vf} = E_{va} - E_{per} + E_{atom} \quad (4)$$

where E_{vf} is vacancy formation energy, E_{va} and E_{per} are the energies of the crystal with and without a vacancy, E_{atom} is the total energy per atom in perfect crystal.

The calculated vacancy formation energy of pure Ni was 1.39 eV , which is close to the experimental value of 1.40 eV [24,25]. Then six kinds of alloying elements were substituted for the Ni atom at the site of N_2 as shown in Fig. 5. Because the effect of solute element on solvent atoms decreases as the increase of distance, only the vacancy formation energy of the first nearest neighbor was calculated and summarized in Table 2.

The calculation results show that the elements slightly increase the energies needed to form a vacancy located in the first nearest neighbor. The effect of vacancy formation energy on the equilibrium concentration of vacancies can be expressed as

$$c_0 = \exp(-E_{vf}/kT) \quad (5)$$

Therefore, these alloying elements can depress the equilibrium concentration of vacancies nearby.

Table 2

The vacancy formation energy of the first nearest neighbor of the alloying elements.

	Alloying element					
	Re	Co	W	Cr	Mo	Ru
$E_{vf} \text{ (eV)}$	1.44	1.42	1.43	1.45	1.41	1.40

Table 3

The migration barriers of the first nearest neighbor vacancies of alloying elements.

	Alloying element					
	Re	Co	W	Cr	Mo	Ru
$E_{mb} \text{ (eV)}$	1.07	1.03	1.16	1.08	1.15	1.20

3.2.2. Vacancy migration energy

The calculated vacancy migration barriers E_{mb} in pure Ni was 1.04 eV , which agrees well with the experimental value of 1.0 eV [26]. A summary of the migration barriers of the vacancy located in the first nearest neighbor of the alloying element is presented in Table 3. The results indicate that the alloying elements Ru, W and Mo can raise the migration barrier of their first nearest neighbor vacancy considerably, as shown in Fig. 6. Cr and Re increase E_{mb} in some sort. It means that the vacancies around these alloying elements must overcome higher barriers to migrate from one equilibrium site to another. Only the element Co reduces E_{mb} , it can improve the ability of the vacancy diffusion when the concentration of vacancies is supersaturated.

The activation energy for vacancy diffusion is defined as follows:

$$E_d = E_{vf} + E_{mb} \quad (6)$$

Therefore, the activation energy for vacancy diffusion in pure Ni is 2.43 eV and the changes of E_d by addition of alloying elements are summarized in Table 4.

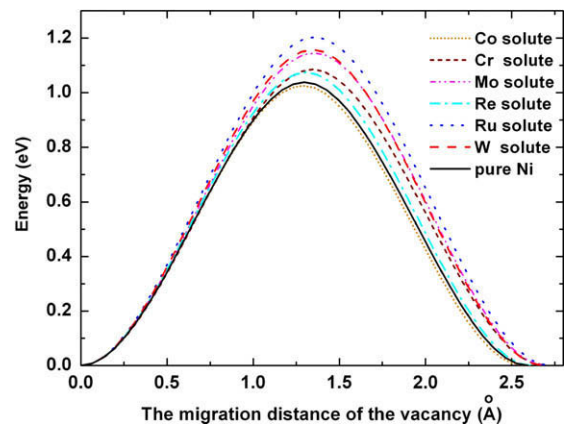


Fig. 6. The changes of the system energies along the path of migration.

Table 4

The influences of alloying elements on the activation energy for vacancy diffusion.

	Alloying element					
	Re	Co	W	Cr	Mo	Ru
$E_d \text{ (eV)}$	2.51	2.45	2.59	2.53	2.56	2.60
$\Delta E_d \text{ (eV)}$	0.08	0.02	0.16	0.10	0.13	0.17

4. The influence of alloying elements on the dislocation climbing velocity

According to the theory of dislocation, the force required for dislocation climb is given by [10]

$$F_m = (E_{vf}/b^2)\sin\psi \quad (7)$$

where b is the length of Burgers vector, ψ is the angle between the dislocation line and the Burgers vector. For dislocations which are not nearly screw, thus for ψ different from zero, the force F_m is close to the magnitude order of the theoretical elastic limit $Gb/10$, where G is the shear modulus. However, a slow motion remains possible by means of vacancies diffusion even though the force applied to the dislocation is much smaller than the F_m .

For a dislocation with edge portion, climb becomes much easier by motions of jogs because the jog can glide along the line by vacancy emission or absorption [27]. Since a perfect dislocation will dissociate into two partial dislocations in FCC structure, the climb of a single partial dislocation would produce an extended surface with high energy. Therefore, a constriction must be formed before a jog moves along the dislocation line, as shown in Fig. 7.

There is a thermodynamic equilibrium number of jogs per unit length of dislocation given by

$$C_j \simeq \exp(-E_j/kT) \quad (8)$$

where E_j is the energy of jog formation, k is Boltzmann constant and T is temperature. Because a jog will increase the energy of a constriction by forming a bending segment in the dislocation line, E_j includes the energy of forming a constriction (E_c), the elastic energy of a jog segment and the atomic misfit in the core of the dislocation [28]. Since the elastic and the misfit energies are small compared with E_c , E_j is given by [29]

$$E_j \simeq E_c = 2 \left[\frac{G\vec{b}_1 \cdot \vec{b}_2}{2\pi} T_l \right]^{1/2} DI(C) \quad (9)$$

where

$$D = \frac{Gb_1^2}{8\pi E_{sf}} \frac{2-v}{1-v} \left(1 - \frac{2v}{2-v} \cos 2\psi \right) \quad (10)$$

T_l is the line tension and $I(C) = 0.53573C$ is the integrating parameter, where

$$C = \cos(\psi + \pi/6)\cos(\psi - \pi/6) + \sin(\psi + \pi/6) \times \sin(\psi - \pi/6)/(1-v) \quad (11)$$

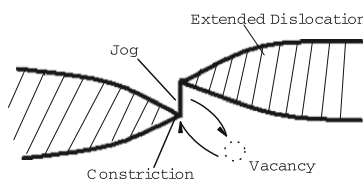


Fig. 7. The moving of a jog along the line by vacancy emission or absorption after the extended dislocation constricts.

v is the Poisson ratio, \vec{b}_1 and \vec{b}_2 are the Burgers vectors of two partial dislocations.

From Eqs. (9) and (10), it can be concluded that the velocity of dislocation climbing is related to the stacking fault energy E_{sf} . In the processing of creep, the dislocation moves very slowly, thus the jog concentration stays near its equilibrium level. The speed of jog movement is controlled by the rate of vacancies diffusion, and the activation energy of jog diffusion can be given by Eq. (6).

Besides the concentration of jogs and the rate of vacancies diffusion, the applied force also influences the speed of dislocation climb. The applied force is expressed as

$$F = F_e + F_s + F_t \quad (12)$$

where F_e is the elastic compression due to external stresses which is given by

$$F_e = b\sigma_n \quad (13)$$

where σ_n is the normal stress perpendicularity to the climb plane. F_s is the chemical force only considered if there is a supersaturation of vacancies, and F_t is the line tensile force which is important when the curvature of dislocation line is small. Because F_s and F_t are small compared with F_e except in special cases, these two items are neglected in this paper.

As indicated above, the rate of a dislocation climbing is

$$v = nbC_jP_j = nbv_0 \exp\left[-\frac{E_j}{kT}\right] \exp\left[-\frac{E_d - \sigma_n b^3}{kT}\right] \quad (14)$$

where n is the number of positions into which the vacancy can jump, P_j is the diffusion probability of a jog, and v_0 is the vibrational frequency of the jog. The activation energy of dislocation climbing is defined as

$$E = E_j + E_d - \sigma_n b^3 \quad (15)$$

and put the values in Tables 1 and 4 into Eq. (14). The Debye frequency of Ni and 1 GPa are chosen as the values of v_0 and σ_n . The relationship among the dislocation climbing velocity, temperature, alloying element and dislocation character is shown in Fig. 8.

Fig. 8 suggests that from the approximate screw dislocation (for ψ approaching 0°) to absolute edge dislocation as ψ increasing, the velocity of dislocation climbing decreases remarkably. Besides, the climb of dislocation is inhibited by addition of alloying elements. The extent of hampering effect varies with element since different elements exert different influences on E_{sf} and E_d . Interestingly, the order of inhibiting ability among elements is $W > Mo > Ru > Re > Cr > Co$ when ψ approaching 0° and $\psi = 30^\circ$; however, the order turns to $Mo > W > Re > Ru > Cr > Co$ when $\psi = 60^\circ$ and $\psi = 90^\circ$. It means that the influences of alloying elements on dislocation climbing velocity depend on the characters of dislocations. From Eqs. (9)–(11), it can be seen that E_j relays on ψ , whereas E_d does not. Take the elements Re and Ru for example, because Re-resolution has a smaller E_{sf} , the disparities of E_j between Re-resolution and Ru-resolution become more with the

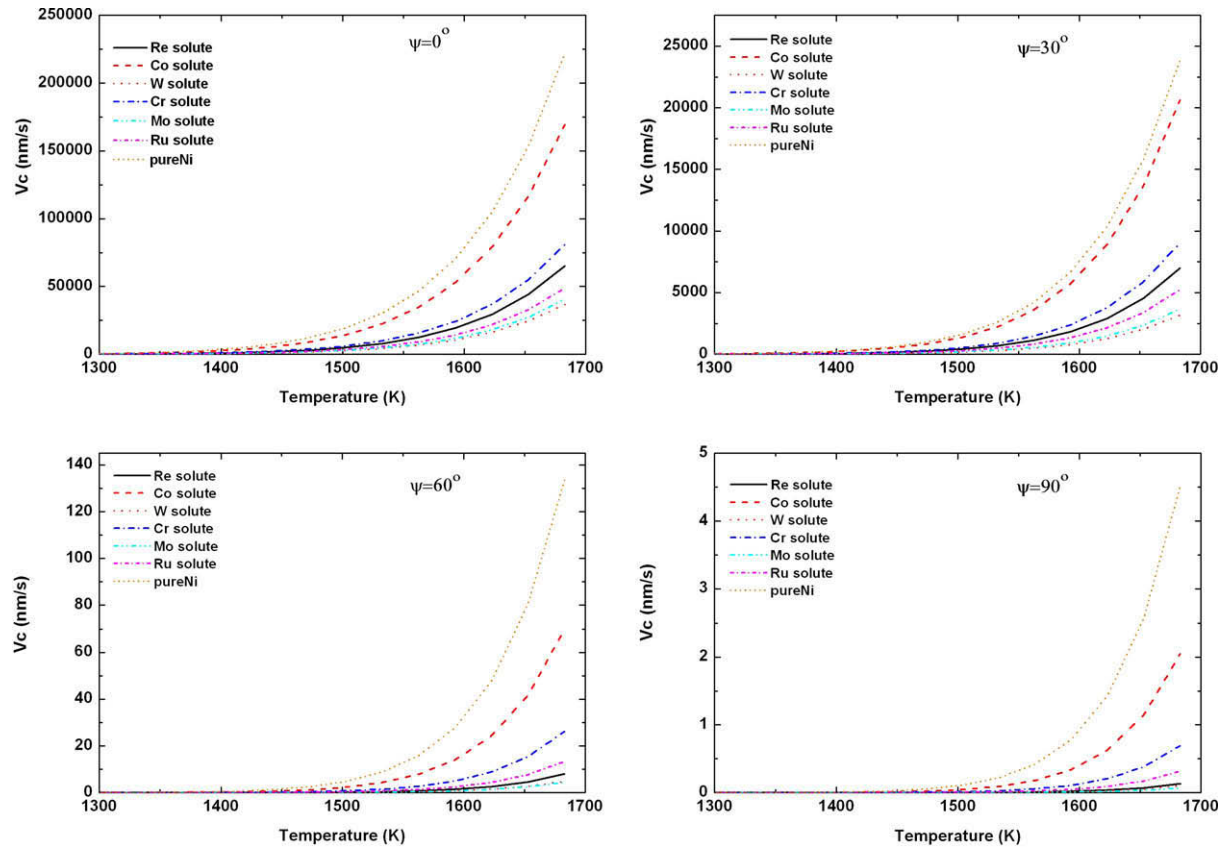


Fig. 8. The relationship among the velocity of dislocation climbing, temperature, solute elements and ψ .

increase of ψ and result in the reversion of order of the activation energy of dislocation climbing, as shown in Table 5, $E(\text{Re}) < E(\text{Ru})$ when $\psi = 30^\circ$ and $E_j(\text{Re}) - E_j(\text{Ru}) = 0.08$ eV. Nevertheless, $E(\text{Re}) > E(\text{Ru})$ when $\psi = 60^\circ$ and $E_j(\text{Re}) - E_j(\text{Ru}) = 0.16$ eV.

5. Conclusions

First principles electronic structure calculations, using the projector augmented wave method and the spin-polarized generalized gradient approximation, was used to study the influences of alloying elements on the velocity of dislocation climbing. The SFE and diffusion activation energy in Ni-based solid solution were calculated, respectively.

Mo, Re and W are found to decrease the stacking fault energy of Ni remarkably. A correlation between the accumulation of electrons and the value of stacking fault energy

exists, the formation of bonding between the alloying element and the Ni atom can reduce the energy of SF region resulting in a low value of SFE. The strong bondings of Re–Ni, Mo–Ni and W–Ni attribute to d–d orbits hybridization between solute atom and Ni.

The alloying elements change the vacancy formation energy in Ni and raise the vacancy diffusion barrier, thus they can increase the activation energy and inhibit the diffusion process of vacancies, especially the elements Ru, W and Mo.

The activation energy of dislocation climbing in Ni-based solid solution was calculated in a extended dislocation model. The results suggest that the alloying elements can suppress the velocity of dislocation climbing by raising both the formation energy and the diffusion activation energy of the jog. The influences of alloying elements on dislocation climbing velocity depend on the characters of dislocations because E_j relies on ψ .

Table 5

The jog formation energy (eV) and the activation energy of dislocation climbing changes with ψ in Ni-based solutions.

ψ ($^\circ$)	Re		Co		W		Cr		Mo		Ru	
	E_j	E	E_j	E	E_j	E	E_j	E	E_j	E	E_j	E
0	0.58	2.99	0.50	2.86	0.58	3.07	0.52	2.95	0.59	3.05	0.53	3.03
30	0.92	3.33	0.80	3.15	0.92	3.41	0.82	3.25	0.94	3.40	0.84	3.34
60	1.83	4.24	1.59	3.94	1.82	4.31	1.63	4.07	1.86	4.32	1.67	4.17
90	2.40	4.81	2.08	4.43	2.39	4.89	2.14	4.57	2.44	4.90	2.18	4.69

Acknowledgement

The work is supported by 973 Project (Ministry of Science and Technology of China, Grant No. 2006CB605102).

References

- [1] Pollock TM, Argon AS. *Acta Metall Mater* 1992;40:1.
- [2] Guo ZX. The deformation and processing of structural materials. Cambridge, England/Boca Raton (FL): Woodhead Publishing/CRC Press; 2005.
- [3] Pollock TM, Field RD. In: Nabarro FRN, Duesbery MS, editors. *Dislocation in solids*. Amsterdam: Elsevier; 2002.
- [4] Warren PJ, Cerezo A, Smith GDW. *Mater Sci Eng A* 1998;250:88.
- [5] Reed RC, Yeh AC, Tin S, Babu SS, Miller MK. *Scr Mater* 2004;51:327.
- [6] Reed RC. *The superalloys fundamentals and applications*. Cambridge University Press; 2006.
- [7] McLean D. *Met Rev* 1962;7:481.
- [8] Weertman J. *AIME Met Soc Trans* 1965;233:2069.
- [9] Guo Z, Miodownik AP, Saunders N, Schille J-Ph. *Scr Mater* 2006;54:2175.
- [10] Friedel J. *Dislocations*. Pergamon Press; 1964.
- [11] Ma S, Carroll L, Pollock TM. *Acta Mater* 2007;55:5802.
- [12] Kremer M, Fu CL, Janotti A, Reed RC. *Acta Mater* 2005;53:2369.
- [13] Kresse G, Hafner J. *Phys Rev B* 1993;47:558.
- [14] Kresse G, Furthmüller J. *Phys Rev B* 1996;54:11169.
- [15] Blochl PE. *Phys Rev B* 1994;50:17953.
- [16] Kresse G, Joubert D. *Phys Rev B* 1999;59:1758.
- [17] Perdew JP, Burke K, Ernzerhof M. *Phys Rev Lett* 1996;77:3865.
- [18] Monkhorst HJ, Pack JD. *Phys Rev B* 1976;13:5188.
- [19] Murr LE. *Interfacial phenomena in metals and alloys*. Reading (MA): Addison Wesley; 1975.
- [20] Carter CB, Hoimes SM. *Philos Mag* 1977;35:1161.
- [21] Henkelman G, Jóhannesson G, Jónsson H. In: *Progress on theoretical chemistry and physics*. Dordrecht: Kluwer Academic Publishers; 2000.
- [22] Henkelman G, Uberuaga BP, Jónsson H. *J Chem Phys* 2000;113:9901.
- [23] The implementations of the CI-NEB for VASP. <<http://theory.cm.utexas.edu/henkelman>>.
- [24] Seeger A, Schumacher D, Schilling W, Diehl J. *Vacancies and interstitials in metals*. Amsterdam: North-Holland; 1970.
- [25] Wycisk W, Feller-Kniepmeier M. *J Nucl Mater* 1978;69/70:616.
- [26] Osipov KA. *Activation processes in solid metals and alloys*. New York: American Elsevier; 1964.
- [27] Hull D, Bacon DJ. *Introduction to dislocations*. 3rd ed. Pergamon Press; 1984.
- [28] Stroh AN. *Proc Phys Soc Lond Sec B* 1954;67:427.
- [29] Wang CY, Liu SY, Han LG. *Phys Rev B* 1990;41:1359.